CHAPTER TEN

The Use of HyPer to Examine Spatial and Temporal Changes in H_2O_2 in High Light-Exposed Plants

Marino Exposito-Rodriguez[*,1], Pierre Philippe Laissue[*,1], George R. Littlejohn[†], Nicholas Smirnoff[†], Philip M. Mullineaux[*,2]
[*]School of Biological Sciences, University of Essex, Colchester, United Kingdom
[†]Biosciences, College of Life and Environmental Sciences, University of Exeter, Exeter, United Kingdom
[1]These authors contributed equally
[2]Corresponding author: e-mail address: mullin@essex.ac.uk

Contents

Abstract

Exposure of photosynthetic cells of leaf tissues of *Arabidopsis thaliana* (Arabidopsis) to high light intensities (HL) may provoke a rapid rise in hydrogen peroxide (H_2O_2) levels in chloroplasts and subcellular compartments, such as peroxisomes, associated with photosynthetic metabolism. It has been hypothesized that when H_2O_2 is contained at or near its site of production then it plays an important role in signaling to induce acclimation to HL. However, should this discrete containment fail and H_2O_2 levels exceed the

Methods in Enzymology, Volume 527
ISSN 0076-6879
http://dx.doi.org/10.1016/B978-0-12-405882-8.00010-6
© 2013 Elsevier Inc.
All rights reserved.

capacity of antioxidant systems to scavenge them, then oxidative stress ensues which triggers cell death. To test this hypothesis, the spatiotemporal accumulation of H_2O_2 needs to be quantified in different subcellular compartments. In this chapter, preliminary experiments are presented on the use of Arabidopsis seedlings transformed with a nuclear-encoded cytosol-located yellow fluorescent protein-based sensor for H_2O_2, called HyPer. HyPer allows ratiometric determination of its fluorescence at two excitation wavelengths, which frees quantification of H_2O_2 from the variable levels of HyPer *in vivo*. HyPer fluorescence was shown to have the potential to provide the necessary spatial, temporal, and quantitative resolution to study HL responses of seedlings using confocal microscopy. Chlorophyll fluorescence imaging was used to quantify photoinhibition of photosynthesis induced by HL treatment of seedlings on the microscope staging. However, several technical issues remain, the most challenging of which is the silencing of HyPer expression beyond the seedling stage. This limited our pilot studies to cotyledon epidermal cells, which while not photosynthetic, nevertheless responded to HL with 45% increase in cytosolic H_2O_2.

1. INTRODUCTION

1.1. Hydrogen peroxide and signaling in response to changes in light intensity

In common with all nonphotosynthetic aerobic eukaryotic cells, plants produce and accumulate hydrogen peroxide (H_2O_2) and other reactive oxygen species (ROS) at different times and in different subcellular locations. In addition, plant and algal cells produce ROS as a byproduct of photosynthesis in chloroplasts (Galvez-Valdivieso & Mullineaux, 2010; Suzuki, Koussevitzky, Mittler, & Miller, 2012; Waring, Klenell, Bechtold, Underwood, & Baker, 2010) and processes allied to this, such as the photorespiratory cycle, which results in production of millimolar quantities of H_2O_2 in peroxisomes (Costa et al., 2010; Queval et al., 2007). Many perturbations of photosynthesis promote H_2O_2 production of which one of the most studied is exposure to fluctuating light intensity (Galvez-Valdivieso & Mullineaux, 2010; Pogson, Woo, Förster, & Small, 2008; Suzuki et al., 2012). Sudden exposure to very high light intensities (often called excess light, EL) can provoke irreversible photoinhibition caused by the rapid accumulation of ROS, including H_2O_2, in chloroplasts. This leads to oxidative damage to the photosynthetic apparatus, which can trigger cell death. Visibly, this is often manifested as the bleaching of leaf tissues and production of discrete microscopic lesions (Karpinski et al., 1999; Mühlenbock et al., 2008; Mullineaux & Baker, 2010). Lesion formation is partly due to direct

tissue damage but mostly by the initiation of programmed cell death initiated by the accumulation of ROS in the chloroplast (Kim et al., 2012; Mullineaux & Baker, 2010).

Under moderate increases in light intensity, typically <10-fold over growth light intensity (referred to as high light; HL), which elicit largely reversible photoinhibition and initiation of acclimation to HL (Mullineaux & Baker, 2010). H_2O_2 accumulation in leaf tissues also occurs, but in a more specific manner. In *Arabidopsis thaliana* (Arabidopsis) under HL, H_2O_2 accumulation was detected primarily in the chloroplasts of bundle sheath cells (BSCs), which are located adjacent to the vascular parenchyma (VP; Fryer et al., 2003; Galvez-Valdivieso et al., 2009). In addition, H_2O_2 was detected in the apoplast of BSCs, possibly dismutated from superoxide anion produced in a reaction catalyzed by plasma membrane-associated NADPH oxidases. NADPH oxidase activity was stimulated by the hormone abscisic acid (ABA) whose synthesis was activated in the VP in a HL- and humidity-dependent manner. It was proposed that H_2O_2 produced in BSC chloroplasts augmented this ABA signal allowing HL responses from multiple chloroplasts present in this cell type to be integrated into a single signal transduction pathway (Galvez-Valdivieso et al., 2009; Galvez-Valdivieso & Mullineaux, 2010; Mullineaux & Baker, 2010).

1.2. A spatial component to H_2O_2 signaling

From the above studies, it was hypothesized that the H_2O_2-initiated signaling from BSC chloroplasts may be converted to a non-ROS signal so that signal transduction could traverse the reducing environment of the cytosol (Galvez-Valdivieso & Mullineaux, 2010; Mullineaux, Karpinski, & Baker, 2006). The alternative view is that H_2O_2 may diffuse out of chloroplasts and accumulate in a localized manner to trigger a cytosol-based signaling system (Mubarakshina et al., 2010; Mullineaux et al., 2006). This might occur in a manner similar to the localized accumulation of H_2O_2 for signal transduction in microdomains associated with microbody membranes and plasma membranes of mammalian cells challenged with growth factors or by wounding (Ushio-Fukai, 2006; Woo et al., 2010) and perhaps also the containment and Ca^{2+}-associated signaling associated with H_2O_2 scavenging in plant peroxisomes (Costa et al., 2010). In general terms, when such containment of H_2O_2 occurs in plant cells, it was suggested that signaling would lead to an acclimation in response to changes in the environment. In contrast, a general diffusion of H_2O_2 away from its site of production to sufficient levels

to promote oxidative damage could trigger cell death-associated signaling (Mullineaux & Baker, 2010; Mullineaux et al., 2006). However, observations with isolated chloroplasts and protoplasts have suggested that H_2O_2 can potentially leak out of chloroplasts in a light intensity-dependent manner (Mubarakshina et al., 2010). These observations suggest that H_2O_2 could act directly as a retrograde signal from the chloroplast to possibly activate regulatory proteins such as the protein phosphatase 2C isoform ABI2 (Miao et al., 2006) and/or heat shock transcription factors implicated in HL responses (Miller & Mittler, 2006; Nishizawa-Yokoi et al., 2011).

To answer these important questions it has become imperative to determine at the subcellular level in plant cells and tissues, the spatial and temporal patterns of the accumulation of H_2O_2 and other ROS in response to changes in light intensity and other environmental perturbations. In this chapter, we describe some of the problems to be overcome and technical developments needed to carry out further research.

1.3. Methods currently used for H_2O_2 localization

Of all the ROS, H_2O_2 is the most stable (Halliwell & Gutteridge, 1999) and can be estimated by a variety of methods based on acid extraction from tissues (Queval, Hager, Gakière, & Noctor, 2008). However, the major drawback of these methods is that they are limited for temporal resolution and completely lack any spatial resolution. Fluorescent and colorimetric chemical dyes used for detection of ROS allow high spatial resolution using microscopic imaging techniques. However, a critical review concluded that none can be used without very careful assessment of artifacts and that most measure what they term "reactive species," that is, various forms of ROS and reactive nitrogen species (e.g., nitric oxide, peroxynitrite) (Halliwell & Whiteman, 2004). For H_2O_2 dye probes, it is evident that the currently used methods suffer from a number of disadvantages (Snyrychova, Ferhan, & Eva, 2009). These problems include the degree of chemical specificity (fluorescein- and rhodamine-based compounds), the influence of peroxidase activity (Amplex Red, 2′,3′-diaminobenzidine [DAB]), degree of toxicity (DAB, Amplex Red), and the sacrifice of tissue (DAB, cerium trichloride). However, there is a more universal problem; all the probes react irreversibly with H_2O_2 so that they provide poor temporal resolution. This is because oxidized probe accumulates and takes time to dissipate. Related to this problem, none of these dye-based methods indicate the concentration of peroxide. Indeed, accumulation of highly fluorescent

oxidized probe could even be giving a false impression that high H_2O_2 concentrations occur in plant cells.

1.4. HyPer, a GFP-based genetically encoded biosensor for H_2O_2

The recent development of genetically encoded green fluorescent protein (GFP)-based sensors has made it possible to develop powerful methods for monitoring noninvasively the dynamics of small molecules and atoms *in vivo*. In principle, GFP sensors allow excellent subcellular and spatiotemporal resolution, with sensitivities in the nanomolar to millimolar range and are reversible in their interactions with their targets (Markvicheva et al., 2011; Okumoto, Alexander, & Frommer, 2012). GFP-based probes have been successfully used *in planta* and have simplified measurements of Ca^{2+} (YC3.6; Krebs et al., 2011; Monshausen, Messerli, & Gilroy, 2008), cellular redox state (RoGFP; Meyer & Brach, 2009), pH (pHusion; Gjetting, Ytting, Schulz, & Fuglsang, 2012), and the hormone auxin (DII-VENUS; Brunoud et al., 2012). The development of a sensor for H_2O_2 named HyPer, has changed the situation completely for measuring the *in vivo* concentrations of this molecule (Belousov et al., 2006; Markvicheva et al., 2011). HyPer consists of the regulatory domain of an *Escherichia coli* (*E. coli*) transcription factor OxyR, which is used by this bacterium to monitor H_2O_2 levels (Choi et al., 2001), inserted into a circularly permuted yellow fluorescent protein (cpYFP; Nagai, Sawano, Park, & Miyawaki, 2001). A pair of redox-active cysteine residues in the OxyR domain of HyPer is located in a hydrophobic pocket, accessible only to amphiphilic molecules such as H_2O_2 and inaccessible to charged oxidants such as superoxide anion or reactive nitrogen species such as nitric oxide and peroxynitrite (Belousov et al., 2006). Importantly, the excitation spectrum of HyPer has two maxima (420 and 500 nm) which show differential changes in fluorescence emission (516 nm) after oxidation. Both forms can be visualized by laser excitation in a confocal system or with widefield fluorescence microscopy. The measurement of emission at two excitation maxima means that the redox state of HyPer can be determined ratiometrically. This allows the calculation of a dimensionless value, which avoids artifacts associated with differences in the levels of HyPer expression. This is important as HyPer levels will vary from cell to cell, tissue to tissue, and transgenic line to transgenic line and avoids issues where cells move. In summary, the properties of the H_2O_2-sensing domain of HyPer, dictate a high selectivity of the probe, high sensitivity and, importantly, good reversibility in the

intracellular environment (Belousov et al., 2006; Malinouski, Zhou, Belousov, Hatfield, & Gladyshev, 2011).

The ability of HyPer to report increases in H_2O_2 *in vivo* has been demonstrated in *E. coli*, mammalian cells (Belousov et al., 2006) and in the wound response of zebrafish larvae (Niethammer, Grabher, Look, & Mitchison, 2009). In plant cells, Costa et al. (2010) presented the first and successful expression of HyPer in the cytoplasm and peroxisomes of Arabidopsis and tobacco cells. The authors demonstrated that the fluorescent ratio of cytosolic HyPer (cHyPer) changes upon the addition of exogenous H_2O_2 and was proportional to the amount of H_2O_2 applied. There was clear dose dependence in guard cells of epidermal peels indicating that HyPer appears to be a useful tool to measure the real-time *in vivo* spatiotemporal dynamics of H_2O_2 accumulation in plant cells.

One limitation of HyPer, that is not uncommon for GFP-based sensors (e.g., Pericam and RoGFP; Jiang et al., 2006; Nagai et al., 2001; Schwarzländer et al., 2012), is for potential artifacts to arise due to the pH sensitivity of the fluorescence which can mimic a significant part of its H_2O_2-sensing range (Belousov et al., 2006; Choi, Swanson, & Gilroy, 2012). Therefore, the local pH must be measured in each particular experiment. This is especially the case when the biosensor is targeted to a subcellular compartment where a change in pH can be anticipated, such as the chloroplast stroma in response to light. pH measurements could be made separately using a pH-sensitive dye (Niethammer et al., 2009) or dual imaging using a genetically encoded pH sensor to control this potential artifact and allow the calculation of H_2O_2 levels corrected for alterations in pH. However, in our initial experiments we have confined ourselves to measuring changes in cHyPer fluorescence in HL-exposed cells. This is because the cytosol of plant cells has been shown to maintain pH homeostasis by possession of a high passive buffering capacity. This has been demonstrated by the absence of cytosolic pH fluctuations in cells challenged with external pH changes and where apoplastic pH changed drastically (Gjetting et al., 2012). Consequently, for the purposes of our initial experiments, the effects of pH on HyPer fluorescence were assumed to be minimal for this subcellular compartment.

1.5. Silencing of HyPer expression in plant tissues

A problem that has been observed in some genetically encoded biosensors in plant tissues is a weak or absent fluorescence. For example, the glucose

sensors based on the CFP–YFP pair, which has been used to measure steady state glucose levels in mammalian cells, showed transgene silencing in Arabidopsis transformants (Deuschle et al., 2006). Furthermore, an early version of the calcium sensor Yellow Cameleon used to determine [Ca^{2+}] dynamics expressed only in guard cells (Allen et al., 1999). That guard cells did not display a suppression of fluorescence suggests that posttranscriptional gene silencing (PTGS) might be playing a role. This is because guard cells are symplastically isolated from surrounding tissues and do not receive gene silencing signals from their neighbors through plasmodesmata (Himber, Dunoyer, Moissiard, Ritzenthaler, & Voinnet, 2003). This hypothesis was supported by using *sgs3* and *rdr6* transgene-silencing mutants, defective in PTGS (Mourrain et al., 2000; Peragine, Yoshikawa, Wu, Albrecht, & Poethig, 2004) to eliminate silencing of the glucose sensor genes, resulting in high fluorescence levels. The use of transgene-silencing mutants, however, is not ideal because they show phenotypic differences from the wild type and could complicate the interpretation of data.

2. EXPERIMENTAL PROCEDURES

2.1. In planta expression pattern of cytosolic HyPer (cHyPer)

A binary Ti plasmid carrying 35S:cHyPer was introduced into *Agrobacterium tumefaciens* strain GV3101:pMP90. In anticipation of potential gene silencing problems (see Section 1.5), *Arabidopsis sgs3–11* plants (Mourrain et al., 2000) were transformed with the *Agrobacterium* strain using standard procedures (Clough & Bent, 1998). In addition, a cHyPer expressed in *Arabidopsis* wild type (ecotype Col-0) was used and was kindly provided by Dr. Alex Costa (Costa et al., 2010). Seedlings were grown in peat-based compost in a controlled environment under an 8/16-h light/dark cycle at a photosynthetically active photon flux densities (PPFD) of 150 μmol m^{-2} s^{-1}, 22 ± 1 °C temperature, and relative humidity of 50%.

The seedlings expressing cHyPer were imaged with confocal laser scanning microscopy to analyze cHyPer fluorescence (Fig. 10.1). A strong fluorescence signal of cHyPer in epidermal cells, with a clear cytosolic and nuclear signal (Fig. 10.2C), was easily detected in both wild type and *sgs3–11* transgenic lines at 7 days from the date of sowing and including a 3-day stratification treatment of seeds at 4 °C to synchronize germination. Fluorescence was limited to cotyledons (stage 1.0; cotyledons fully opened; Boyes et al., 2001). No cHyPer fluorescence signal was detected in

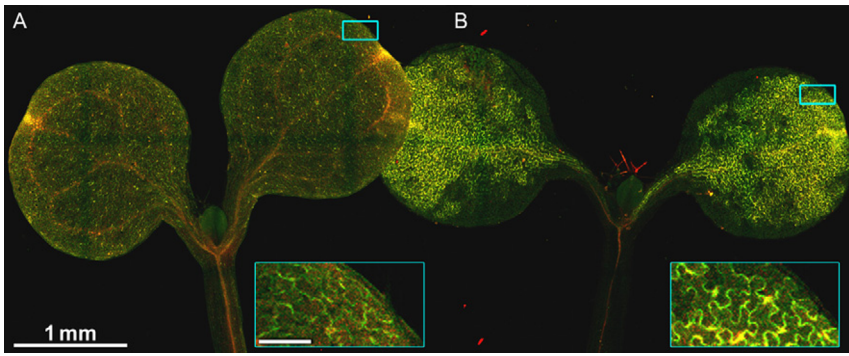

Figure 10.1 Expression of cytosolic HyPer (cHyPer) in 8-day-old *Arabidopsis* seedlings. (A) cHyPer in wild type. (B) cHyPer in *sgs3–11* background. The seedlings were placed next to each other on the same slide, ensuring image acquisition conditions were identical. Inset cyan rectangles show epidermal cells at higher magnification (scale bar: 100 μm).

epidermal cells from roots or hypocotyls. However, from day 8, HyPer fluorescence in plants with wild-type background diminished, becoming dim and patchy (Fig. 10.1A). This problem was attenuated by using *Arabidopsis* mutant *sgs3–11* (Fig. 10.1B). The onset of silencing in seedlings of these mutants occurs much later, between days 12 and 15 (stage 1.02; rosette leaves >1 mm in length). After this time, no signal was detected in epidermal cells of cotyledons or rosette leaves in the mutant.

2.2. Mounting live seedlings for experimental manipulation

To ensure that cHyPer can dynamically report H_2O_2 within cotyledon epidermal cells, we performed pilot experiments using live cell imaging. Live microscopy at high spatial and temporal resolution depends on appropriate immobilization of the specimen. To evaluate the amplitude of the HyPer response to H_2O_2 added to intact epidermal cells, we designed two procedures to add solutions and measure H_2O_2 changes without affecting cell viability. For the first assay, a seedling was placed in a 35 mm petri dish with a #1.5 coverslip glass-bottom (ibidi GmbH, D-82152 Martinsried), covered with a mesh (Fig. 10.2A) and glued down on the sides using rubber cement ("Fixogum," Marabuwerke GmbH, D-71732 Tamm), gently pressing the seedling against the coverslip. The dish was filled with 200 μL of water and H_2O_2 solution dropped directly onto the water to obtain a final concentration of 1 m*M*. In the second procedure, the seedlings were mounted in a custom-built perfusion chamber to achieve exchange of H_2O_2 solution. Microscope slides were covered with 24×40 mm #1.5 coverslips (Agar Scientific, Essex, UK), placed so as to form a cross, and attached with

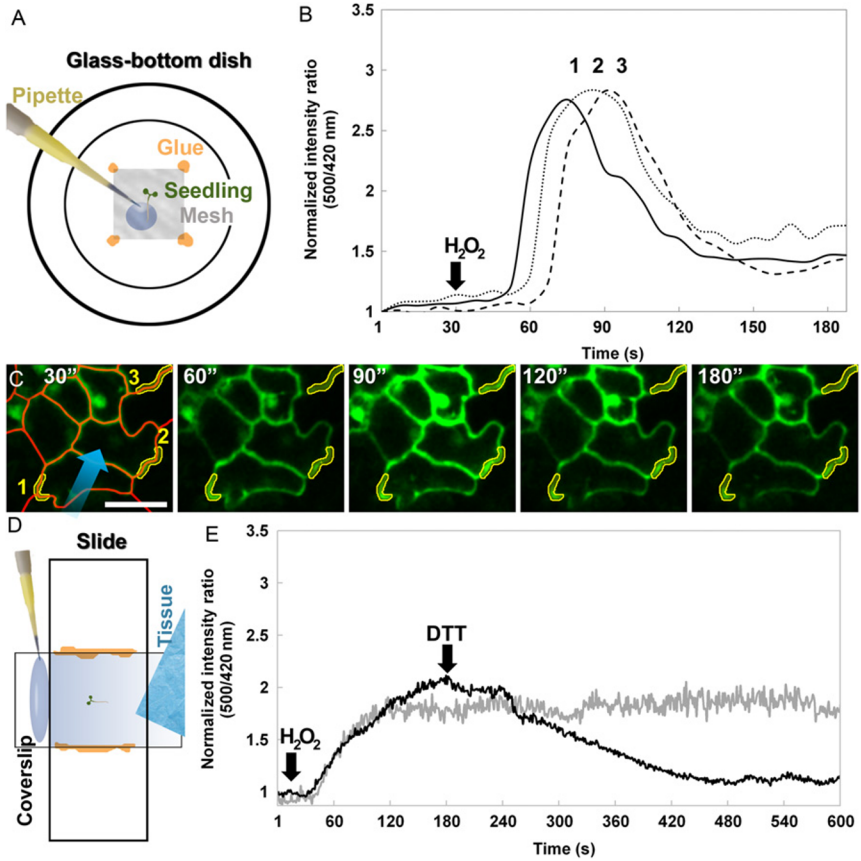

Figure 10.2 Cytosolic HyPer (cHyPer) response to added H_2O_2 in cotyledon epidermal cells. (A) Experimental setup using 35 mm glass-bottom petri dishes. (B) Time course of HyPer response to H_2O_2 addition (arrow). 1, 2, and 3 indicate the maxima in regions of interest, indicated in (C). (C) Image sequence of cotyledon epidermal cells expressing cHyPer. Only the green channel (excitation at 500 nm) is shown. Cells were exposed to 1 m*M* H_2O_2. A blue arrow shows the general direction of H_2O_2 flux. Time is indicated in the bottom right. Numbers 1, 2, 3 indicate the positions of the analyzed regions of interest. Cell borders are overlaid in red. Scale bar: 10 μm. (D) Slide-based experimental setup using custom-built perfusion chamber. (E) Time course of redox changes in cHyPer after the addition of H_2O_2 (1 m*M*) and the reducing agent dithiothreitol (DTT; 1 m*M*) using the experimental setup indicated in (D). All ratio values were normalized to a minimum value of 1.0.

double-sided adhesive tape (Fig. 10.2D). As the coverslip sticks out at one end, solution can be positioned on it. Using a tissue at the other end of the coverslip, the liquid is sucked into the space between slide and coverslip and moves across by capillary force.

2.3. HyPer dynamics in epidermal cells

The first assay using glass-bottom petri dishes allows the analysis of HyPer at high temporal resolution in single cells. Cellular response after the addition of H_2O_2 was rapid (~30 s, Fig. 10.2B). Ratios decreased in the same amount of time, but did not fall to the same levels as before H_2O_2 addition. This may be because exogenous H_2O_2 remained present in the media surrounding the seedling after the addition. Around threefold increase of the cHyPer ratio (500/420 nm) in epidermal cells was observed using saturating amounts of H_2O_2 (1 m*M*) (Fig. 10.2B). This agrees with the maximum value of the HyPer dynamic range determined earlier (Belousov et al., 2006; Markvicheva et al., 2011). This assay enabled the recording of the cHyPer response in three different cells (Fig. 10.2C) at high temporal resolution, allowing the determination of the direction and rate of H_2O_2 diffusion. The second assay showed different H_2O_2 dynamics (Fig. 10.2D). Response was slow and sustained, and took almost 3 min to reach a maximum. These values were lower compared to the first assay, only reaching a ratio increase of around 1.8-fold. After H_2O_2 treatment, addition of the reducing agent dithiothreitol (1 m*M*) confirmed the reversible proprieties of HyPer in this system (Fig. 10.2E). Interestingly, although the initial kinetics in both systems were different, the steady state signal values attained by both mounting methods were very similar after 2 min.

2.4. Confocal microscopy

A flow chart detailing the steps of image acquisition, processing and analysis is shown in Fig. 10.3. It is important that optimized samples are acquired respecting several criteria. First, saturated pixels should be avoided, as they may represent lost information and cannot be used for quantification. Look-up tables color-coding the maximum greyscale value, commonly implemented in microscope image acquisition software, allowed the detection of saturated pixels by adjusting laser power and/or detector gain to avoid them. Second, if temporal resolution was essential (as used in the

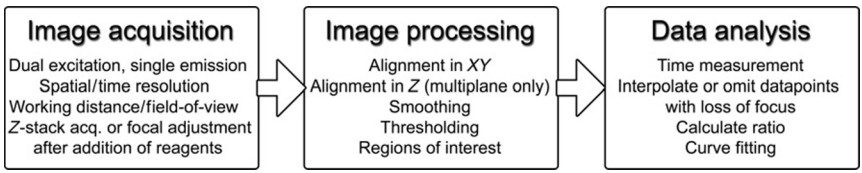

Figure 10.3 Flow chart summarizing the different steps and approaches to be considered.

glass-bottom dish assay), an image size of 256 × 256 pixels offered sufficient spatial information while greatly reducing acquisition time, allowing for ~1 frame/s using unidirectional scanning. Spectral information was separated using line scanning rather than full-frame mode. For higher spatial resolution (for slide-based assays), an image size of 512 × 512 pixels was used.

For image acquisition, a Nikon A1si confocal microscope was used with the following objectives: a CFI 10× Plan Fluor with numerical aperture (NA) 0.3, a CFI 20× Plan Apochromat violet-corrected (VC) with NA 0.75, and a CFI 60× Plan Apochromat VC oil-immersion objective with NA 1.4. Images were acquired using one-way sequential line scans of two excitation lines, with laser power at 405 nm between 15 and 33 arbitrary units (AU), and at 488 nm between 7 and 17 AU, and emission collected with one detector at 540/30 nm, with a photomultiplier tube gain of 90–120 AU. Differential interference contrast images were acquired using the transmitted light detector at a gain of 80–120 AU. No offset was used, and pinhole size was set between 1.2 and 2 times the Airy disk size of the used objective, depending on signal strength. Axial step size was 0.8–1.6 μm, with three image planes per *z*-stack.

2.5. Image processing and analysis

Invariably, samples move in the three spatial dimensions (*X*, *Y*, and *Z*) upon the addition of solutions to the media. Lateral movement in *X* and *Y* was corrected in one channel using the translational mode of the StackReg algorithm (Thévenaz, Ruttimann, & Unser, 1998) in ImageJ (Rasband, 1997), and the stored shift matrix applied to the other channel. Color separation using line scans ensured nearly zero temporal deviation between the channels. Alignment was validated by 3D visual inspection of fiduciary marks in overlaid channels. *Z*-movement was corrected by acquiring three image planes along the *Z*-axis, and the appropriate planes were selected and combined postacquisition. Alternatively, rapid manual adjustment of the focal plane after the addition of a solution was carried out and yielded good results.

For measurement of fluorescent intensity, a previous approach for ratiometry was expanded (Schwarzländer et al., 2008). Images were first smoothed using a Gaussian filter with 3 × 3 kernel size. Bright structures were then segmented in NIS-Elements (version 3.21.03, build 705 LO). The aim was to restrict measurement to brightly fluorescing structures only. Segmentation was done using the "define binary" command, smoothing and cleaning the binary area once. Thresholding was assessed by visual

inspection. Within the segmented datasets, regions of interest were used, providing a second layer for restricting measurements. This allowed measuring and comparing fluorescent signals in different parts of the imaged area Fig. 10.2.

3. PILOT EXPERIMENTS USING HL STRESS

3.1. Experimental setup

HL was applied to seedlings mounted on the microscope stage. The tungsten lamp, usually used for bright field illumination, was adapted for light treatments by adjusting the field diaphragm, in order to deliver a small, brightly illuminating circular beam. This enabled application of white light to single cotyledons only (Fig. 10.4A). Intensity was measured with a light meter (SKP200, Skye, Powys, UK). The cotyledon was exposed to HL with PPFDs of 1200, 1600, and 2000 $\mu mol\ m^{-2}\ s^{-1}$. The spectrum of the light emitted from the tungsten lamp at different intensities was further assessed using a spectroradiometer (SR9910, Macam, Livingstone, UK) (Fig. 10.4B).

3.2. Chlorophyll fluorescence imaging

To ensure that illumination was locally contained, and to determine the effects that light of different PPFDs had on the photoinhibition of cotyledons, chlorophyll fluorescence (Cf) parameters were measured using a Fluorimager chlorophyll fluorescent imaging system (Fluorimager; Technologica Ltd., Colchester, Essex, UK). For the theory and use of Cf to measure photosynthetic efficiency, the reader is referred to Baker (2008). A decline in the Cf parameter F_v/F_m, which describes the maximum quantum efficiency of photosystem II photochemistry (Baker, 2008), was used to indicate the degree of photoinhibition suffered by cotyledons exposed to HL (Fig. 10.4C). The first cotyledon of each seedling was not treated with HL, serving as control with imaged F_v/F_m values around 0.76. Increasing light intensities on the second cotyledon caused a progressive decrease in F_v/F_m after 20 min in a light intensity-dependent manner (Fig. 10.4C).

3.3. Pilot experiment

The light intensity that caused a decrease in F_v/F_m of ca. 20% (PPFD 1200 $\mu mol\ m^{-2}\ s^{-1}$) was used to image the fluorescence of cHyPer in *sgs3–11* cotyledons before, during, and after exposure to HL. The two

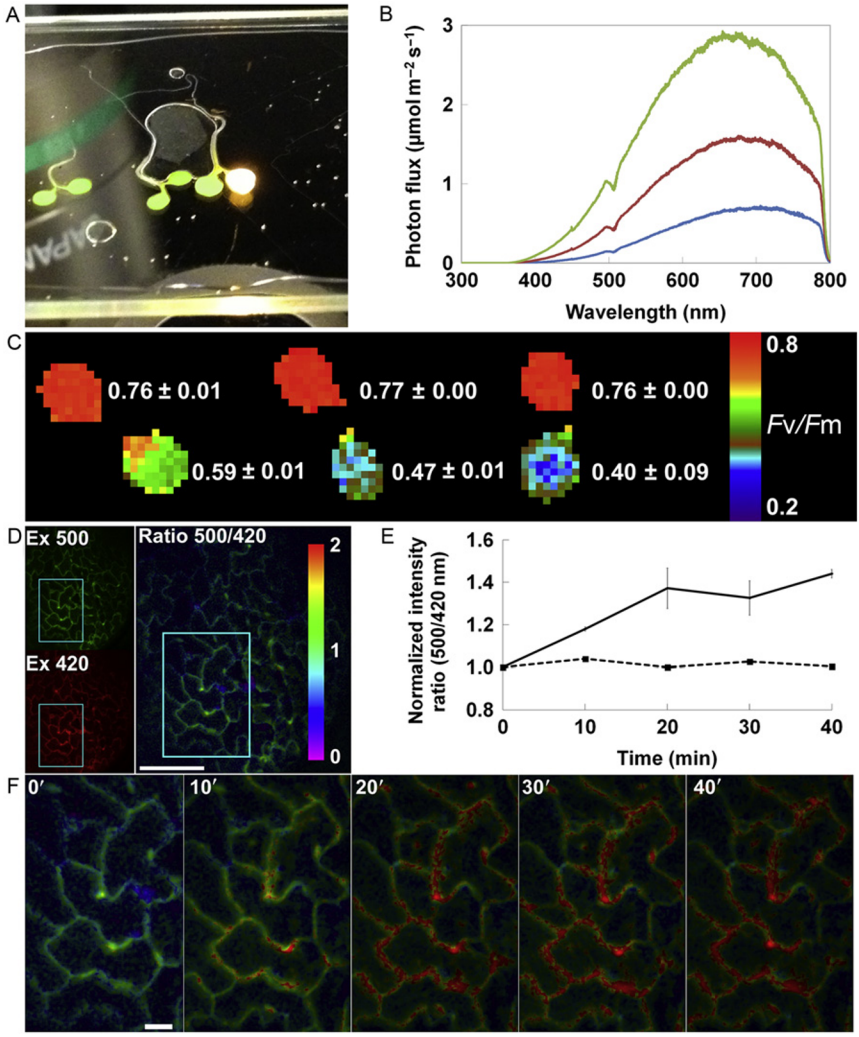

Figure 10.4 Pilot experiment inducing high light stress on the confocal microscope. (A) A precise, small area of light was applied to only one cotyledon. (B) Spectral measurement of the light used in this study. (C) Fluorescence images of cotyledons showing F_v/F_m values after 20 min exposures at 1200, 1600, and 2000 μmol m^{-2} s^{-1} (left to right, respectively). (D) Combining the two channels to produce a ratiometric image. The inset cyan rectangles demarcate the enlarged area shown in (F). (E) cHyPer response of cotyledon after high light treatments in 10 min intervals. Time point zero is a low light (LL) value taken immediately prior to exposure of the cotyledon to HL. Solid line and dashed line are values from cotyledons exposed to HL or LL parallel control, respectively. Values are the means (±SD; $n = 3$). All ratios were normalized to a minimum value of 1.0. (F) False-color ratio images corresponding to (E).

channels (excitation at 500 nm, green channel, and excitation at 420 nm, red channel) were combined and visualized as ratio images using a false-color scale (Fig. 10.4D). Using the slide-based setup described in Section 2.2, a fluorescence image of a seedling's cotyledon, grown in conditions described in Section 2.1, was taken (defined as time point zero). The cotyledon was then exposed to HL for 20 min. Light was then switched off, and a fluorescence image taken every 10 min over 40 min. After exposure to HL, the fluorescence intensity ratio of cHyper in epidermal cells increased by a maximum of 45% compared to time point zero (Fig. 10.4E).

4. CONCLUSIONS

From these preliminary experiments, it is clear that HyPer can provide the necessary spatial, temporal, and quantitative resolution to study HL responses and the compartmentation of H_2O_2 at the subcellular level. However, before experiments to examine the accumulation and diffusion of H_2O_2 in HL-exposed cells' photosynthetic tissues of true leaves, the silencing of HyPer expression has to be overcome and robust methods for codetermination of pH changes also have to be instigated. If these technical issues can be overcome, then HyPer holds out the prospect of giving us many more insights into the behavior of H_2O_2 in HL-exposed cells. This is clear from the preliminary data present in Fig. 10.4 in that HL triggers an accumulation of H_2O_2 in cotyledon epidermal cells and even more once the light has been switched off (Fig. 10.4E and F). This observation is remarkable because these cells do not contain chloroplasts.

ACKNOWLEDGMENTS

We thank Dr. Alex Costa for the cHyPer/Col-0 line used in this study. The authors are grateful to the UK Biotechnology and Biological Sciences Research Council (BBSRC) for the support of this research (Grant Number BB/I020071/1).

REFERENCES

Allen, G. J., Kwak, J. M., Chu, S. P., Llopis, J., Tsien, R. Y., Harper, J. F., et al. (1999). Cameleon calcium indicator reports cytoplasmic calcium dynamics in Arabidopsis guard cells. *The Plant Journal*, *19*, 735–747.

Baker, N. R. (2008). Chlorophyll fluorescence: A probe of photosynthesis in vivo. *Annual Review of Plant Biology*, *59*, 89–113.

Belousov, V. V., Fradkov, A. F., Lukyanov, K. A., Staroverov, D. B., Shakhbazov, K. S., Terskikh, A. V., et al. (2006). Genetically encoded fluorescent indicator for intracellular hydrogen peroxide. *Nature Methods*, *3*, 281–286.

Boyes, D. C., Zayed, A. M., Ascenzi, R., McCaskill, A. J., Hoffman, N. E., Davis, K. R., et al. (2001). Growth stage-based phenotypic analysis of Arabidopsis: A model for high throughput functional genomics in plants. *The Plant Cell*, *13*, 1499–1510.

Brunoud, G., Wells, D. M., Oliva, M., Larrieu, A., Mirabet, V., Burrow, A. H., et al. (2012). A novel sensor to map auxin response and distribution at high spatio-temporal resolution. *Nature*, *482*, 103–106.

Choi, H., Kim, S., Mukhopadhyay, P., Cho, S., Woo, J., Storz, G., et al. (2001). Structural basis of the redox switch in the OxyR transcription factor. *Cell*, *105*, 103–113.

Choi, W.-G., Swanson, S. J., & Gilroy, S. (2012). High-resolution imaging of Ca^{2+}, redox status, ROS and pH using GFP biosensors. *The Plant Journal*, *70*, 118–128.

Clough, S. J., & Bent, A. F. (1998). Floral dip: A simplified method for Agrobacterium-mediated transformation of *Arabidopsis thaliana*. *The Plant Journal*, *16*, 735–743.

Costa, A., Drago, I., Behera, S., Zottini, M., Pizzo, P., Schroeder, J. I., et al. (2010). H_2O_2 in plant peroxisomes: An in vivo analysis uncovers a $Ca^{(2+)}$-dependent scavenging system. *The Plant Journal*, *62*, 760–772.

Deuschle, K., Chaudhuri, B., Okumoto, S., Lager, I., Lalonde, S., & Frommer, W. B. (2006). Rapid metabolism of glucose detected with FRET glucose nanosensors in epidermal cells and intact roots of Arabidopsis RNA-silencing mutants. *The Plant Cell*, *18*, 2314–2325.

Fryer, M. J., Ball, L., Oxborough, K., Karpinski, S., Mullineaux, P. M., & Baker, N. R. (2003). Control of *Ascorbate Peroxidase 2* expression by hydrogen peroxide and leaf water status during excess light stress reveals a functional organisation of *Arabidopsis* leaves. *The Plant Journal*, *33*, 691–705.

Galvez-Valdivieso, G., Fryer, M. J., Lawson, T., Slattery, K., Truman, W., Smirnoff, N., et al. (2009). The high light response in *Arabidopsis* involves ABA signaling between vascular and bundle sheath cells. *The Plant Cell*, *21*, 2143–2162.

Galvez-Valdivieso, G., & Mullineaux, P. M. (2010). The role of reactive oxygen species in signaling from chloroplasts to the nucleus. *Physiologia Plantarum*, *138*, 430–439.

Gjetting, K. S., Ytting, C. K., Schulz, A., & Fuglsang, A. T. (2012). Live imaging of intra- and extracellular pH in plants using pHusion, a novel genetically encoded biosensor. *Journal of Experimental Botany*, *63*, 3207–3218.

Halliwell, B., & Gutteridge, J. M. C. (1999). *Free radicals in biology and medicine* (3rd ed.). Oxford, UK: Oxford University Press.

Halliwell, B., & Whiteman, M. (2004). Measuring reactive species and oxidative damage in vivo and in cell culture: How should you do it and what do the results mean? *British Journal of Pharmacology*, *142*, 231–255.

Himber, C., Dunoyer, P., Moissiard, G., Ritzenthaler, C., & Voinnet, O. (2003). Transitivity-dependent and -independent cell-to-cell movement of RNA silencing. *The EMBO Journal*, *22*, 4523–4533.

Jiang, K., Schwarzer, C., Lally, E., Zhang, S. B., Ruzin, S., Machen, T., et al. (2006). Expression and characterization of a redox-sensing green fluorescent protein (reduction–oxidation-sensitive green fluorescent protein) in Arabidopsis. *Plant Physiology*, *141*, 397–403.

Karpinski, S., Reynolds, H., Karpinska, B., Wingsle, G., Creissen, G., & Mullineaux, P. (1999). Systemic signaling and acclimation in response to excess excitation energy in Arabidopsis. *Science*, *284*, 654–657.

Kim, C., Meskauskiene, R., Zhang, S., Lee, K.-P., Asok, M. L., Blajecka, K., et al. (2012). Chloroplasts of *Arabidopsis* are the source and a primary target of a plant-specific programmed cell death signaling pathway. *The Plant Cell*, *24*, 3026–3039.

Krebs, M., Held, K., Binder, A., Hashimoto, K., DenHerder, G., Parniske, M., et al. (2011). FRET-based genetically encoded sensors allow high-resolution live cell imaging of Ca^{2+} dynamics. *The Plant Journal*, *69*, 181.

Malinouski, M., Zhou, Y., Belousov, V. V., Hatfield, D. L., & Gladyshev, V. N. (2011). Hydrogen peroxide probes directed to different cellular compartments. *PLoS One*, *6*(1), e14564. http://dx.doi.org/10.1371/journal.pone.0014564.

Markvicheva, K. N., Bilan, D. S., Mishina, N. M., Gorokhovatsky, A. Y., Vinokurov, L. M., Lukyanov, S., et al. (2011). A genetically encoded sensor for H_2O_2 with expanded dynamic range. *Bioorganic & Medicinal Chemistry*, *19*, 1079–1084.

Meyer, A. J., & Brach, T. (2009). Dynamic redox measurements with redox-sensitive GFP in plants by confocal laser scanning microscopy. *Methods in Molecular Biology*, *479*, 93–107.

Miao, Y. C., Lv, D., Wang, P. C., Wang, X. C., Chen, J., Miao, C., et al. (2006). An *Arabidopsis* glutathione peroxidase functions as both a redox transducer and a scavenger in abscisic acid and drought stress responses. *The Plant Cell*, *18*, 2749–2766.

Miller, G., & Mittler, R. (2006). Could heat shock transcription factors function as hydrogen peroxide sensors in plants? *Annals of Botany*, *98*, 279–288.

Monshausen, G. B., Messerli, M. A., & Gilroy, S. (2008). Imaging of the Yellow Cameleon 3.6 indicator reveals that elevation in cytosolic Ca^{2+} following oscillating increases in growth in root hairs of Arabidopsis. *Plant Physiology*, *147*, 1690–1698.

Mourrain, P., Béclin, C., Elmayan, T., Feuerbach, F., Godon, C., Morel, J. B., et al. (2000). Arabidopsis *SGS2* and *SGS3* genes are required for posttranscriptional gene silencing and natural virus resistance. *Cell*, *101*, 533–542.

Mubarakshina, M. M., Ivanov, B. N., Naydov, I. A., Hillier, W., Badger, M. R., & Krieger-Liszkay, A. (2010). Production and diffusion of chloroplastic H_2O_2 and its implication to signaling. *Journal of Experimental Botany*, *61*, 3577–3587.

Mühlenbock, P., Szechynska-Hebda, M., Plaszczyca, M., Baudo, M., Mateo, A., Mullineaux, P. M., et al. (2008). Chloroplast signaling and *LESION SIMULATING DISEASE1* regulate crosstalk between light acclimation and immunity in Arabidopsis. *The Plant Cell*, *20*, 2339–2356.

Mullineaux, P. M., & Baker, N. R. (2010). Oxidative stress: Antagonistic signaling for acclimation or cell death? *Plant Physiology*, *154*, 521–525.

Mullineaux, P. M., Karpinski, S., & Baker, N. R. (2006). Spatial dependence for hydrogen peroxide-directed signaling in light-stressed plants. *Plant Physiology*, *141*, 346–350.

Nagai, T., Sawano, A., Park, E. S., & Miyawaki, A. (2001). Circularly permuted green fluorescent proteins engineered to sense Ca^{2+}. *Proceedings of the National Academy of Sciences of the United States of America*, *98*, 3197–3202.

Niethammer, P., Grabher, C., Look, A. T., & Mitchison, T. J. (2009). A tissue-scale gradient of hydrogen peroxide mediates rapid wound detection in zebrafish. *Nature*, *459*, 996–999.

Nishizawa-Yokoi, A., Nosaka, R., Hayashi, H., Tainaka, H., Maruta, T., Tamoi, M., et al. (2011). HsfA1d and HsfA1e involved in the transcriptional regulation of *HsfA2* function as key regulators for the Hsf signaling network in response to environmental stress. *Plant & Cell Physiology*, *52*, 933–945.

Okumoto, S., Alexander, J., & Frommer, W. B. (2012). Quantitative imaging with fluorescent biosensors. *Annual Review of Plant Biology*, *63*, 663–706.

Peragine, A., Yoshikawa, M., Wu, G., Albrecht, H. L., & Poethig, R. S. (2004). *SGS3* and *SGS2/SDE1/RDR6* are required for juvenile development and the production of trans-acting siRNAs in Arabidopsis. *Genes & Development*, *18*, 2368–2379.

Pogson, B. J., Woo, N. S., Förster, B., & Small, I. D. (2008). Plastid signaling to the nucleus and beyond. *Trends in Plant Science*, *13*, 602–609.

Queval, G., Hager, J., Gakière, B., & Noctor, G. (2008). Why are literature data for H_2O_2 contents so variable? A discussion of potential difficulties in the quantitative assay of leaf extracts. *Journal of Experimental Botany*, *59*, 135–146.

Queval, G., Issakidis-Bourguet, E., Hoeberichts, F. A., Vandorpe, M., Gakière, B., Vanacker, H., et al. (2007). Conditional oxidative stress responses in the Arabidopsis

photorespiratory mutant *cat2* demonstrate that redox state is a key modulator of daylenghth-dependent gene expression, and defined photoperiod as a crucial factor in the regulation of H_2O_2-induced cell death. *The Plant Journal*, *52*, 640–657.

Rasband, W. S. (1997) ImageJ. U. S. National Institutes of Health, Bethesda, Maryland.

Schwarzländer, M., Fricker, M. D., Müller, C., Marty, L., Brach, T., Novak, J., et al. (2008). Confocal imaging of glutathione redox potential in living plant cells. *J Microsc*, *231*(2), 299–316.

Schwarzländer, M., Murphy, M. P., Duchen, M. R., Logan, D. C., Fricker, M. D., Halestrap, A. P., et al. (2012). Mitochondrial 'flashes': A radical concept repHined. *Trends in Cell Biology*, *22*, 503–508.

Snyrychova, I., Ferhan, A., & Eva, H. (2009). Detecting hydrogen peroxide in leaves in vivo—A comparison of methods. *Physiologia Plantarum*, *135*, 1–18.

Suzuki, N., Koussevitzky, S., Mittler, R., & Miller, G. (2012). ROS and redox signaling in the response of plants to abiotic stress. *Plant, Cell & Environment*, *35*, 259–270.

Thévenaz, P., Ruttimann, U. E., & Unser, M. (1998). A pyramid approach to subpixel registration based on intensity. *IEEE Trans Image Process*, *7*, 27–41.

Ushio-Fukai, M. (2006). Localizing NADPH oxidase-derived ROS. *Science Signaling*, *2*, re8.

Waring, J., Klenell, M., Bechtold, U., Underwood, G. J. C., & Baker, N. R. (2010). Light-induced responses of oxygen photoreduction, reactive oxygen species production and scavenging in two diatom species. *Journal of Phycology*, *46*, 1206–1217.

Woo, H. A., Yim, S. H., Shin, D. H., Kang, D., Yu, D.-Y., & Rhee, S. G. (2010). Inactivation of peroxiredoxin I by phosphorylation allows localized H_2O_2 accumulation for cell signaling. *Cell*, *140*, 517–528.

The author has requested enhancement of the downloaded file. All in-text references underlined in blue are l